



On numerical moment-curvature relationship of a beam

D PANDIT^{1,*} and BHAKTI N PATEL²

¹Department of Civil Engineering, IEST, Shibpur, Howrah, West Bengal 711103, India

²Department of Mechanical Engineering, Parul Institute of Engineering and Technology, Parul University, Waghodia, Vadodara, Gujarat 391760, India
e-mail: debojyoti@civil.iests.ac.in

MS received 16 June 2021; revised 22 September 2021; accepted 3 November 2021

Abstract. In complex bending problems involving material and geometric non-linearity, quite often moment-curvature based approach is preferred over stress-strain based methods. For such an approach, available uniaxial stress-strain test data or models are required to be converted into moment-curvature relationship. The process of conversion of uniaxial stress-strain relationship into a moment-curvature relationship is non-unique. And hence, complete moment-curvature law can be modelled suiting any of the several hardening laws. Such modelling will be very important when a beam is under cyclic load producing reverse plastic deformation. In this paper, an approach is presented to obtain a unique moment-curvature relationship from any given stress-strain law. Standard elasto-plastic models viz. elastic-perfectly plastic, isotropic and kinematic hardening are considered to produce corresponding unique moment-curvature relationships. The results indicate that an isotropic curvature hardening model, corresponding to an elastic perfectly plastic stress-strain model, would be erroneous. Additionally, step by step procedure of using the approach in solving a large deflection elasto-plastic beam problem, is demonstrated here.

Keywords. Moment-curvature; large deflection; elastic perfectly plastic; isotropic hardening; kinematic hardening; non-linear equation; elasto-plastic deformation.

1. Introduction

Beams are one of the most important structural members that are primarily meant to transfer bending load. The research on beam mechanics is an ever expanding field. The problem of beam bending that is of research interest is almost exclusively non-linear in nature; arising from material and/or geometric non-linearity. The research on beam mechanics can be broadly classified into numerical and analytical approaches. In the last couple of decades, most of the analytical and semi analytical methods developed to solve the non-linear bending problems, correspond to techniques adapted from elliptic integrals, series expansion, homotopy perturbation etc. and can be found in [1–5] and the references therein.

On the front of purely numerical methods, the finite element method (FEM) is probably the most successful among others. In this regard, the seminal works of [6, 7] and later by other researchers like [8] in developing fiber beam-column finite elements to solve cyclic non-linear response of RC framed structure is worth consulting. Nevertheless, the search for a beam mechanics specialized, efficient, fast and computationally less expensive means in

comparison to FEM has continued. To develop specialized numerical approaches for solving beams, standard numerical integration schemes are employed. A few noted methods developed for the elastica in recent times are [9–11]. In solving non-linear material problems, noteworthy methods can be found in [12–14] and the references therein. One of the primary motivation for developing non FEM numerical methods is governed by the requirements of a design engineer who needs faster solution and lesser design iterations. In this regard, a higher order beam formulation is developed in [5, 15]. In sheet metal bending industry, the primary focus of the manufacturing process is to obtain the desired bent shape of sheet which has undergone large deflection and is permanently deformed after springback. In these industries, where the computational capacity of the control units are low, such methods are welcome, see [16–18] etc.

Since bending is primarily associated with moment and curvature, many formulations utilise this relationship explicitly, mostly for problems with material non-linearity. A few explicit moment-curvature based approaches that are used to determine damage in flexible structures can be found in [19–21] etc. In structural engineering, inelastic moment-curvature based formulations are employed in the design and analysis of reinforced beam cross-sections,

*For correspondence

some of the important works can be found in [22–25]. A simplified moment-curvature model adapted to simulate non-linear evolution of reduction of moment of inertia in a bridge pier is demonstrated in [26]. In [27] and in [28] a Ludwick type non-linear material model is considered to solve the large deflection beam bending problem using a moment-curvature based approach.

Additionally, in some recent research areas, like in inelastic bending of micro-beam see [29], shape memory simulation of polymeric beam see [30] etc., explicit moment-curvature based approaches are being adopted. The versatility of the moment-curvature approach is thus quite apparent. Further, the inelastic deformation based applications are often associated with cyclic or non-monotonic loading. Since laboratory test results of materials under cyclic loading are generally available for uniaxial stress-strain responses, for application to cyclic inelastic bending processes, it is inconvenient to use such results. In such cases, most often one converts the monotonic inelastic uniaxial stress-strain result or model into an equivalent moment-curvature relationship, depending on the cross-sectional geometry of the beam. This is also because even if test data for bending is available for a beam of a particular material, it won't be useful on a beam made with the same material but with a different cross-sectional shape. However, the problem with this kind of approach is that, the complete moment-curvature response is experimentally unknown and hence its modeling is proposed in a relatively arbitrary manner. For example, in the case of elastic perfectly plastic uniaxial stress-strain model, one analytically obtains curvature hardening in the monotonic moment-curvature response, see [31]. In this case, since there is no hardening at the stress-strain level, the hardening observed at the moment-curvature level, evidently needs imposition of new condition or modeling approach. Very limited literature is available within the scientific community to address the discussed problem in a general way.

The key contribution of the present work is an attempt to circumvent the problem in a generic way without imposing any new assumption or condition. In the present work, complete/cyclic stress-strain law/ data is used to obtain the moment-curvature relationship. In the previous works by the authors, only the monotonic part of the stress-strain law was used to predict the complete/cyclic moment-curvature relationship. In simple words, the paper attempts to obtain a unique moment-curvature relationship, corresponding to any given inelastic or non-linear uniaxial stress-strain model expressed in an incremental form, without imposing any new ad-hoc condition that is originally absent at the stress-strain level. Evidently, in elasto-plastic bending problems where reverse plastic deformation is considerable, such an approach would play an important role. The core idea on which the present paper is based, is quite independent of the type of material model and was first conceived and applied to a shape memory alloy beam and can be found in [32].

Herein, the approach is illustrated considering both rectangular and circular cross-sections and standard elasto-plastic material models. The method is completely explicit¹ in nature unlike elliptic integral solution and is capable of incorporating any material model given in uniaxial stress-strain law form. It may be noted here that the stress-strain law need not be explicit, but the moment-curvature output from the present method will render explicit solution, which is more appealing to the engineering community. The method is also amenable for arbitrarily shaped cross-sections, provided the load acts in a manner producing simple bending without twisting. However, this idea can be extended to beams of arbitrary cross-section under pure bending moments producing bending only in the principal planes of the cross-section. The approach is limited to thin in-extensible beams that follow Euler-Bernoulli hypothesis under small strain condition but may be extended to finite rotation (curvature) cases.

In the following sections, first, the over all solution methodology for a cantilever beam is presented. This is followed by the procedure of obtaining the moment-curvature relationship. The material models in terms of stress and strain, are described after this. Subsequently, the validation of the approach in predicting the monotonic moment-curvature relationship is presented. Following this, the validation of the method is established by comparing the prediction of deflected profiles with finite element method. Next sections include results on cyclic moment-curvature and end force-displacement responses. Lastly, the paper is terminated with apt concluding remarks.

2. Method

The method introduced here is to directly obtain the cyclic moment-curvature response from a uniaxial law without imposing any new modelling assumption. In order to achieve this, the key consideration adopted here is to divide the beam cross-section into even number of imaginary layers in the depth direction and assuming that the uniaxial stress-strain law to be valid only at the centroid of the layers. The outcome of this approach is that, due to increment in curvature, every centroid line will experience increment in strain, which owing to the uniaxial stress-strain law will yield an increment in stress. This increment in stress for a particular layer will account for increment in moment about the centroid of the beam cross-section. All such increments in moment, from each of the layers, will numerically sum up to the total increment of moment due to the increment in curvature for the beam section. Hence, for a given increment in curvature

¹The developed method is stated to be explicit as; i. an explicit relation is developed between the applied force and the end-displacement which is generally absent in analytical or closed-form solutions obtained from elliptic integral method-based approaches, ii. the developed governing differential equation is linearized and solved using the Runge-Kutta 4th order initial value explicit solver with no iterations involved.

for a section the increment in moment will be obtained. Finally, the numerical tangent modulus may easily be obtained by dividing the increment in total bending moment by the increment in curvature. In this section, the above mentioned procedure is explained by first considering the governing deformation differential equation for an end loaded cantilever beam undergoing finite deflection. Following this, the key ingredient of the approach that is the illustration of the procedure to obtain the numerical moment-curvature relationship is discussed. Finally the pertinent stress-strain based material models are described.

2.1 The beam deformation equation

In figure 1, a horizontal cantilever beam of length L and elastic flexural rigidity EI under end vertical dead load P is shown. The primary deformation entity is the angle $\phi(s)$ made by the tangent at any point s on the beam with the horizontal. Proceeding in a similar fashion as in [31], the governing deflection equation reads:

$$D \frac{\partial^2 \phi}{\partial s^2} + P \cos \phi = 0, \quad 0 \leq s \leq L \quad (1)$$

The boundary conditions are given by:

$$\phi|_{s=0} = 0, \quad \frac{\partial \phi}{\partial s}|_{s=L} = 0 \quad (2)$$

Where, D is the general flexural tangent modulus and for a general rate independent constitutive model for a moment (M)-curvature (κ) based relationship, it is given by:

$$D = \frac{dM}{d\kappa} \quad (3)$$

Clearly, the non linear governing equation given in Eq. 1 can be solved by the incremental procedure as given in [31]. The primary consideration in the procedure involves linearizing the non-linear equation about the current load step. The linearized equation is solved by Runge-Kutta 4th order (RK4) method. In this regard the incremental operator

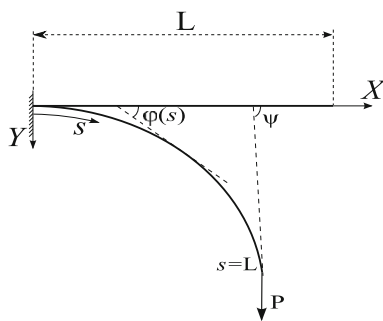


Figure 1. Horizontal cantilever under end vertical dead load P .

$\Delta(\cdot)$ indicates increment with respect to pseudo time t and is given by:

$$\Delta(\cdot) = \frac{\partial(\cdot)}{\partial t} \Big|_t = \frac{\partial(\cdot)}{\partial \psi} \Big|_{\psi(t)} \Delta \psi$$

Here, ψ is the free end angle and indicates the controlling parameter. Keeping all other steps in the procedure same as in [31], in the present work instead of imposing an explicit curvature dependent functional relationship to D , an algorithmic approach is conceived and described in the following section 2.2. Once the solution $\phi(s)$ is obtained after updating, the coordinates of the deflected beam are computed by numerically integrating the following :

$$x(s) = \int_0^s \cos \phi(s) ds; \quad y(s) = \int_0^s \sin \phi(s) ds \quad (4)$$

2.2 The numerical Moment-Curvature relationship

To illustrate the procedure of obtaining D numerically, from a given increment in curvature $\Delta\kappa$, two regular beam cross-sections are considered. A rectangular beam cross-section of width b and depth h is depicted in figure 2b while figure 2a shows a circular beam cross-section of diameter h . Each of the cross-sections is divided into even number of imaginary layers of uniform thickness by solid lines. The natural numbers placed beside are for designating the layers. A dotted line between and parallel to two solid lines indicates the pertinent centroidal axis of that particular layer. The vertical coordinate axis designated by Y (capital Y) is set to originate from the centroid of the entire cross-section.

Clearly, from elementary consideration of mechanics, the increment in bending moment ΔM due to increment in curvature $\Delta\kappa$ of the rectangular section reads:

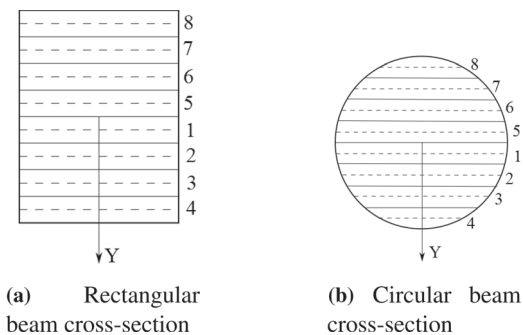


Figure 2. Layering scheme for various beam cross-sections.

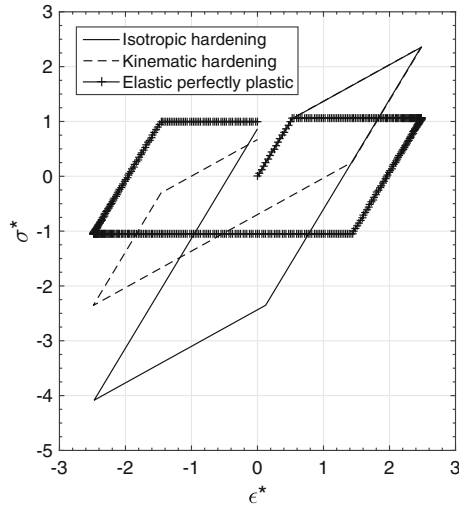


Figure 3. The pictorial representation of the three standard elasto-plastic material models viz. elastic perfectly plastic, isotropic and kinematic hardening laws in terms of normalized uniaxial stress(σ^*)-strain(ϵ^*); $\sigma^* = \frac{\sigma}{\sigma_0}$; $\epsilon^* = \frac{\epsilon}{\frac{2\sigma_0}{E}}$ with $\frac{H}{E} = 0.5$ and $\frac{K}{E} = 0.5$.

$$\Delta M = \int_{-\frac{h}{2}}^{\frac{h}{2}} \Delta \sigma Y b dY \tag{5}$$

And, for the circular cross-section, the above relationship is:

$$\Delta M = \int_{-\frac{h}{2}}^{\frac{h}{2}} \Delta \sigma Y \sqrt{\left(\frac{h}{2}\right)^2 - Y^2} dY \tag{6}$$

Eq. 5 and Eq. 6 can be solved numerically by employing Simpson’s $\frac{1^{rd}}$ rule of integration once increment in stress $\Delta \sigma$ at each of the layers is known. This is computed from the increment in strain $\Delta \epsilon$ and the given material model which is described in detail in section 2.3 . Post determination of ΔM from given $\Delta \kappa$, the flexural tangent modulus, in consideration of Eq. 3, is numerically determined from:

$$D = \frac{\Delta M}{\Delta \kappa} \tag{7}$$

2.3 Incremental material models

As stated in the previous section, to determine ΔM , $\Delta \sigma$ and consequently $\Delta \epsilon$ is required. Now, $\Delta \epsilon$ is obtained from given increment in curvature $\Delta \kappa$ of the section from the “plane section remain plane” condition and is given by:

$$\Delta \epsilon = \Delta \kappa Y \tag{8}$$

The increment in strain $\Delta \epsilon$ thus obtained is used to determine the increment of stress $\Delta \sigma$, by employing the suitable material models. Herein, three standard elasto-plastic material models viz. elastic-perfectly plastic, isotropic and kinematic hardening models are considered. To describe these elasto-plastic material models, the standard terms put to use are as mentioned in the Nomenclature , see [33] for details.

The incremental elastic stress-strain relationship (common for all the material models) reads:

$$\Delta \sigma = E(\Delta \epsilon - \Delta \epsilon^p) \tag{9}$$

To obtain $\Delta \epsilon^p$ yield functions f_j where j index corresponds to the respective material models are defined as:

$$\begin{aligned} f_p &= |\sigma| - (\sigma_0); f_i = |\sigma| - (\sigma_0 + K\alpha); \\ f_k &= |\sigma - q| - (\sigma_0) \end{aligned} \tag{10}$$

Similar to yield function, for an amenable algorithmic approach, plastic load step check functions g_j are introduced where j index corresponds to the particular material model:

$$g_p = g_i = \sigma \Delta \epsilon; g_k = (\sigma - q) \Delta \epsilon \tag{11}$$

The steps presented in algorithm 1 illustrates how to determine ϵ^p from the Eq. 12

Depending on the material model (j) considered, the increment in plastic strain $\Delta \epsilon_j^p$ are given by:

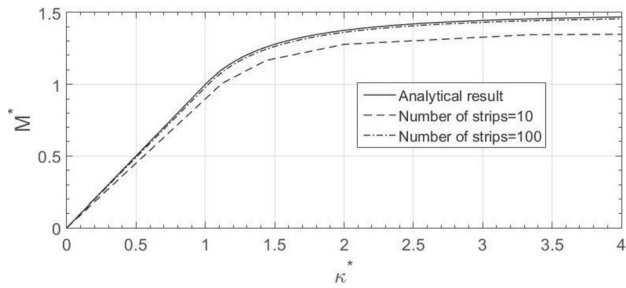
$$\Delta \epsilon_p^p = \Delta \epsilon; \Delta \epsilon_i^p = \frac{E}{E + K} \Delta \epsilon; \Delta \epsilon_k^p = \frac{E}{E + H} \Delta \epsilon; \tag{12}$$

The internal variables are subsequently determined from :

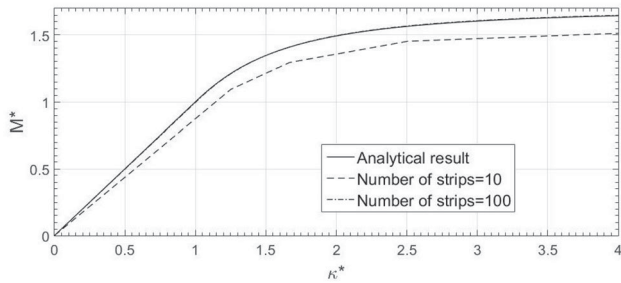
$$\Delta \alpha = |\Delta \epsilon^p|; \Delta q = H \Delta \epsilon^p \tag{13}$$

Algorithm 1: Determination of increment of plastic strain for any model j

Result: $\Delta \epsilon^p$
 Initialization; $\sigma, \epsilon, \epsilon^p, q, \alpha$;
if $f_j = 0$; **and** $g_j > 0$ **then**
 $\Delta \epsilon^p \neq 0$;
 (Determine $\Delta \epsilon^p$ from Eq. 12)
else
 $\Delta \epsilon^p = 0$;
end



(a) Rectangular beam cross-section



(b) Circular beam cross-section

Figure 4. Validation of the approach in predicting moment-curvature responses with analytical elastic-perfectly plastic solutions. Here $M^* = \frac{M}{M_0}$, $\kappa^* = \frac{\kappa}{\kappa_0}$.

It may be noted here that, in consideration of Eqs. 5 and 6, the variables $\sigma, \epsilon, \epsilon_p, \alpha, q$ and functions f_j & g_j ; $j = p, i, k$ are all dependent on the position of the layer along the depth of a beam denoted by Y . It is hence imperative to mention that the variables are functions of pseudo time and Y .

The three material models described here are pictorially depicted in figure 3 under a cyclic strain controlled loading. The magnitude of the material parameters are arbitrarily set at: $\frac{H}{E} = 0.5$ and $\frac{K}{E} = 0.5$.

3. Numerical results and discussion

In this section, moment curvature validation of the developed numerical method with its analytical counterpart is first presented. This is followed by comparing the model's prediction for an end loaded cantilever with the corresponding FEM results obtained using the commercial software ABAQUSTM. Next, moment-curvature responses of rectangular and circular beam cross-sections for the three standard elasto-plastic material models are presented for cyclic curvature loading. Following this, the simulation of the end force-displacement response of a cantilever is presented.

3.1 Validation at the moment-curvature level

For an elastic-perfectly plastic material model, the analytical expression of moment as an explicit function of

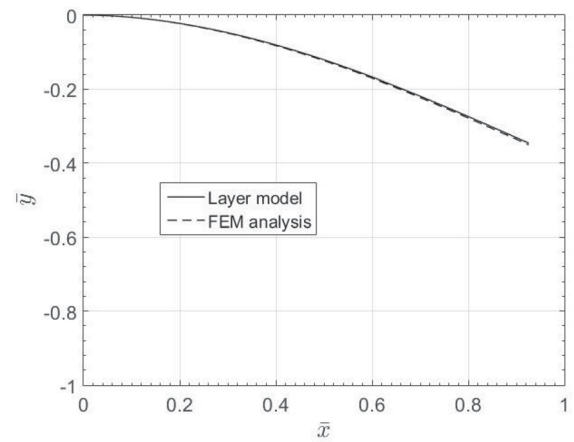


Figure 5. Comparison of deflected profile prediction of present method with FEM (ABAQUSTM) for an end loaded cantilever of elastic-perfectly plastic material model under concentrated vertical dead load P producing elasto-plastic deformation; $\bar{P} = \frac{PL^2}{EI} = 1.11$, $\zeta = \kappa_0 L = 0.77$, fixed end moment $M^* = \frac{M}{M_0} = 1.34$.

curvature under monotonic load can easily be obtained by performing an integration of the model over the beam cross-section. For a rectangular cross-section of width b and depth h , the pertinent relationship is given in [31] as:

$$M^* = \kappa^*, \quad \kappa^* \leq 1$$

$$M^* = \frac{1}{2} \left(3 - \frac{1}{\kappa^{*2}} \right), \quad \kappa^* > 1 \tag{14}$$

Where, moment $M^* = \frac{M}{M_0}$ and curvature $\kappa^* = \frac{\kappa}{\kappa_0}$ are normalized with respect to their initial yield values $M_0 = \frac{bh^2\sigma_0}{6}$ and $\kappa_0 = \frac{2\sigma_0}{Eh}$ respectively. For a circular cross-section of diameter h the above relationship reads: (see Appendix)

$$M^* = \kappa^*, \quad \kappa^* \leq 1$$

$$M^* = \frac{16}{3\pi} \left(1 - \frac{1}{\kappa^{*2}} \right)^{\frac{3}{2}} + \frac{2\kappa^*}{\pi} \left(\alpha - \frac{\sin 4\alpha}{4} \right), \quad \kappa^* > 1; \tag{15}$$

where $\sin \alpha = 1/\kappa^*$. Clearly, from Eqs. 14 and 15 the asymptotic values of normalized moments can be easily obtained to be 1.50 and 1.67 for the rectangular and the circular cross-sections respectively; for large values of normalized curvatures. The validation of the approach in generating accurate moment-curvature response for an elastic-perfectly plastic material can be clearly seen in figure 4. Here it can be seen, that by increasing the number of layers, the predictions converge to the analytical solutions, both for circular and rectangular beam cross-sections. Clearly, for cross-section shapes with known analytical solutions for the monotonic moment-curvature relationship, the number of layers can be decided based on the accuracy desired by comparing with analytical solutions. For shapes

with complicated or unknown closed form expressions, a mesh convergence study may be done to decide on the discretization of the beam in the depth direction.

3.2 Validation at the force-displacement level

In figure 5, the prediction of deflected profile of a cantilever of rectangular cross-section, under a vertical tip dead quasi-static load, made of elastic-perfectly plastic material, employing the present approach, is compared with that of the FEM (ABAQUSTM) simulation. Herein, the elastica parameter² $\zeta = \kappa_0 L = 0.77$ and load $\bar{P} = \frac{PL^2}{EI} = 1.11$, which produced sufficient plastic deformation at the fixed end. From the figure, the prediction is seen to be fair and may be claimed to improve with increase in temporal and spatial discretizations. It is worth pointing out here that the problem is highly non-linear since the deflection is finite and the fixed end moment reached 1.34 times that of its elastic limit which ensures considerable plastic deformation. Further, the time taken by above predictions corresponding to the present approach and FEM simulation are compared to the time taken by the earlier approach (applied to the same cantilever) (as in [31]), and is presented in table 1. It is to be noted that the simulations are carried out for the same time discretization for all the three approaches. Also, the methods are tested on a system with following specifications: Intel(R) Core(TM) i5 CPU M430 @ 2.5GHz, 4GB RAM, 64-bit Operating System. It can be seen that the time taken by the present method is less in comparison to that taken by FEM analysis. However, the present approach is computationally heavy as compared to the earlier one. This is because the present approach is more close to the reality while the earlier one was a simplistic model with more assumptions.

3.3 The moment-curvature responses for various material models

In figure 6, the moment-curvature responses under cyclic curvature controlled loading ensuring reverse plastic deformation, is presented. All the three material models viz. elastic-perfectly plastic, isotropic and kinematic hardening are illustrated for the rectangular as well as for the circular cross-sections. It can be seen that for any given material model, the bending (i.e. moment-curvature) response has similar characteristics for the two cross-sections. Within the limitation of a numerical analysis, it can be claimed that the elastic-perfectly plastic and kinematic hardening material models both yield corresponding near kinematic beam responses. In simple words, in a cyclic moment-curvature response, if the initial yield moment (like stress) point is exceeded by certain amount along the path of increasing curvature loading, then the yield moment point in the

reverse direction happens to be reduced by nearly the same amount. On the other hand, in the case of isotropic material model the beam response shows that the reverse plastic deformation starts at a marginally lower magnitude of moment which is akin to Bauschinger effect, see [35].

3.4 The end force-displacement response

Since the approach developed here is primarily meant for solving a beam deflection problem, which may under go reverse plastic deformation; a cantilever of elastic perfectly plastic material property, under transverse tip dead quasi-static load as shown in figure 1 is considered. As indicated before in 2.1, the controlling parameter to solve Eq.1 is the end angle ψ . It may be pointed out here, that the choice of a kinematic entity over a kinetic quantity as the controlling parameter for solving a differential equation, appeals particularly to problems involving structural softening. Hence an end angle cyclic load with amplitude $\frac{\pi}{6}$ is applied as shown in the inset of figure 7a. The amplitude is chosen arbitrarily ensuring sufficient plastic deformation at the fixed as can be seen in the moment-curvature response of the beam at the fixed end shown in figure 7a. The corresponding end force-displacement response for the cantilever is presented in figure 7b. For comparison with the elastic material, the above mentioned responses are also obtained for the same ψ load with a higher value of yield stress for the beam, such that $\zeta = \kappa_0 L = 2.28$. It may be observed that in both the responses of moment-curvature and end force displacement, the loading and unloading curves do not coincide leading to dissipation loss, typical in elasto-plastic deformation simulations.

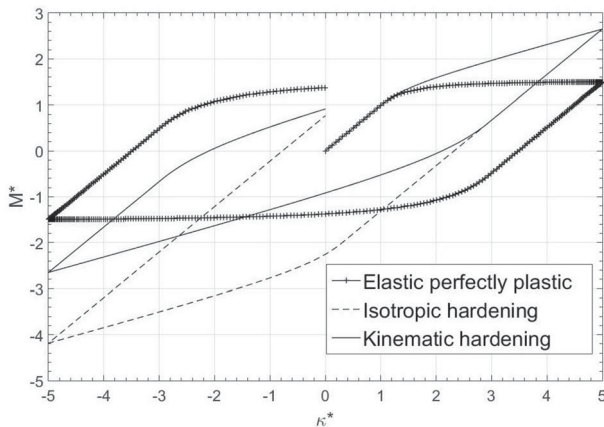
Interestingly, in the unloading phase of moment-curvature curve, the response is linear while in the force-displacement case it is non-linear. This non-linearity is due to the consideration of finite deflection formulation as validated by the elastic response of end force-displacement plot. One of the striking feature of the end force-displacement response is its much smaller area in the enclosed loop in comparison to the moment-curvature plot. This may be attributed to the fact, that the force displacement response, is the over all response of the beam which has a significant length fully elastic, and only a small portion as elasto-plastic. While in the corresponding moment-curvature plot of the fixed end cross-section shown in figure 7a, along the depth of the beam, majority region is under elasto-plastic deformation state for the maximum bending moment produced as compared to its asymptote = 1.50. Additionally, since large deflection is allowed, the bending moment produced at any distance s , measured along the beam is reduced, as against small deflection theory, which in turn reduces plastic deformation for the over all beam.

Another observation worth mentioning is the presence of residual force at the end of the ψ loading cycle, which indicates had there been a force controlled loading cycle,

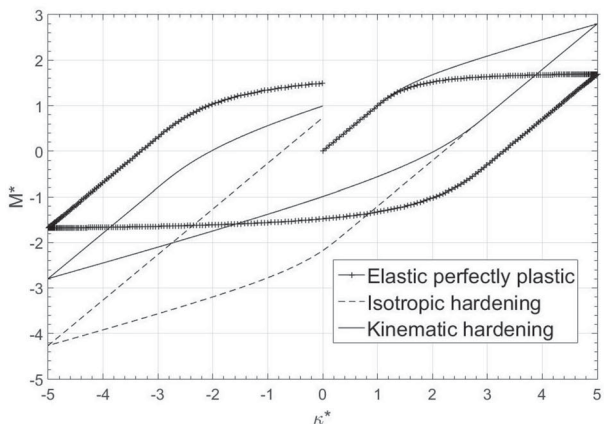
²The details of the elastica parameter can be found in [34].

Table 1. Time comparison for different approaches to solve for cantilever subjected to dead vertical load at the free-end.

	Old Method	Present Method	FEM
Time (in seconds)	0.221	2.98	5.1



(a) Rectangular beam cross-section



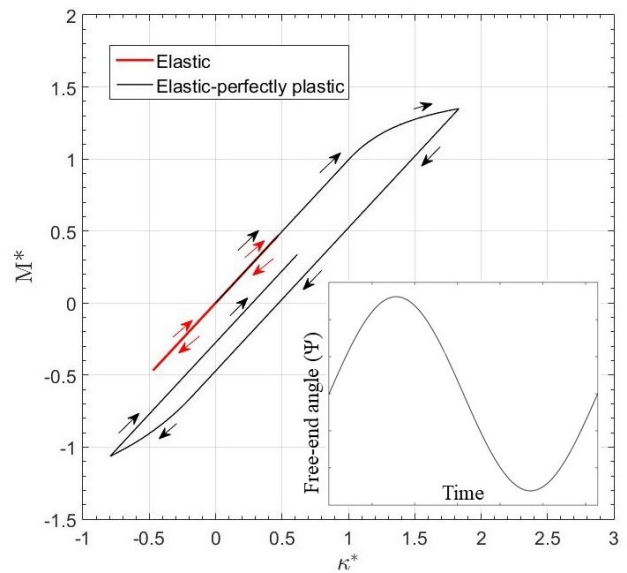
(b) Circular beam cross-section

Figure 6. The moment-curvature responses of rectangular and circular cross-sections for the three standard elasto-plastic material models under sinusoidal curvature (normalized) input of amplitude 5. Here $M^* = \frac{M}{M_0}$, $\kappa^* = \frac{\kappa}{\kappa_0}$.

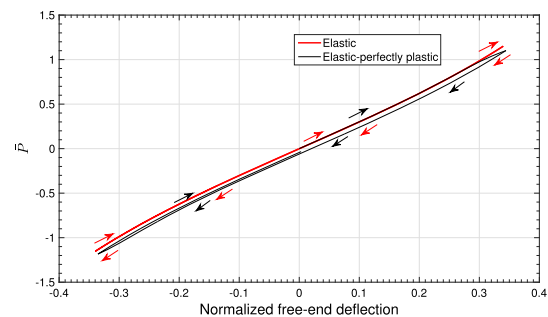
residual deformation corresponding to residual stress would have been produced, conforming to typical elasto-plastic simulation results.

4. Conclusion

In this article, a numerical method to obtain moment-curvature relationship from uniaxial stress-strain law is presented. The method is found to produce more accurate



(a) Normalized moment versus curvature at the fixed end of the cantilever



(b) Force versus end displacement response

Figure 7. Free end force-displacement and corresponding fixed end moment-curvature response of a horizontal cantilever of rectangular cross-section under end vertical non-monotonic normalized load $\bar{P} = \frac{PE^2}{EI}$; normalized displacement $\bar{\delta} = \frac{v(x=L)}{L}$. Here $M^* = \frac{M}{M_0}$, $\kappa^* = \frac{\kappa}{\kappa_0}$. The load is applied by controlling the end angle ψ .

result when the discretization along the cross-section of a beam is increased. One of the key findings of the present work is that, from the elastic-perfectly plastic material model, the obtained moment-curvature response showed near kinematic hardening behaviour. This clearly indicates that it will be grossly wrong, to use an isotropic hardening moment-curvature law for this case, especially when reverse plastic deformation is expected. The applicability of the method in solving a large deflection elasto-plastic problem is successfully demonstrated. However, it may be noted that the approach may be integrated into other kinds of moment-curvature solvers as well, which require the information of the tangent flexural rigidity and moment from curvature input. The approach is claimed to be generic enough to model moment-curvature response of other non-linear material

models like shape memory alloys, shape memory polymers etc when presented in an incremental form. Additionally, the approach may be directly applied to arbitrarily shaped cross-section of beams which bends in any one of the two principal planes. For solving three dimensional bending structural problems, a torque-twist based relationship in addition to the moment-curvature law is required. Such relationships may also be derived in a similar fashion from shear stress-strain data as moment-curvature relationship is derived from uniaxial stress-strain data.

Lastly, the developed approach provides fairly accurate results with less than 1% difference compared to FEM analysis of end displacement under same load. Also, it is shown to be faster and more economical than the FEM analysis and hence it can be implemented in the manufacturing control units with low computational capacity.

Appendix I. Derivation of moment-curvature relationship for a circular cross-section following elastic-perfectly plastic law

In figure 8, the cross-section of area A is assumed to be elastic in the range $-a \leq Y \leq a$ and elasto-plastic outside this range. The total moment M is given by:

$$M = \int_A \sigma Y dA \tag{A1}$$

The above equation corresponding to a circular cross-section reads:

$$M = 4 \int_0^{h/2} \sigma Y \sqrt{\frac{h^2}{4} - Y^2} dY \tag{A2}$$

Using $\sigma = E\epsilon$ and $\epsilon = \kappa Y$ at $Y = a$, a is determined to be:

$$a = \frac{\sigma_0}{E\kappa} \tag{A3}$$

To perform the integration of Eq. A2, it is divided into elastic and elasto-plastic regions as given by:

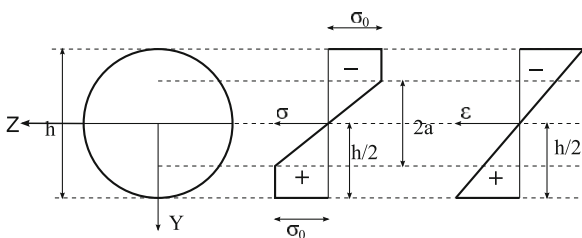


Figure 8. The stress and strain state of a typical solid circular cross-section following elastic-perfectly plastic law.

$$M = 4E\kappa \int_0^a Y^2 \sqrt{\frac{h^2}{4} - Y^2} dY + 4\sigma_0 \int_a^{h/2} Y \sqrt{\frac{h^2}{4} - Y^2} dY \tag{A4}$$

Using the following substitution: $Y = \frac{h}{2} \sin \theta$, Eq.A3 and pertinent normalization, the above equation simplifies into Eq. 15.

Nomenclature

- E Young’s modulus
- H Kinematic hardening modulus
- K Plastic modulus
- σ_0 Initial yield stress
- ϵ^p Plastic strain
- q Back stress
- α Non-negative internal hardening variable
- f_j Yield function; the subscript index $j = p, i, k$ indicate elastic perfectly plastic, isotropic and kinematic hardening models respectively

Declarations

Conflict of interest The authors declare that they have no conflict of interest.

References

- [1] Ghosh S and Roy D 2007 Numeric-analytic form of the adomian decomposition method for two-point boundary value problems in nonlinear mechanics. *Journal of engineering mechanics*, 133(10): 1124–1133
- [2] Banerjee, A Bhattacharya B and Mallik A K 2008 Large deflection of cantilever beams with geometric non-linearity: Analytical and numerical approaches. *International Journal of Non-Linear Mechanics*, 43(5): 366–376
- [3] Maleki Mohammad, Tonekaboni Seyed Ali Madani and Abbasbandy Saeid 2014 A homotopy analysis solution to large deformation of beams under static arbitrary distributed load. *Applied Mathematical Modelling*, 38(1): 355–368
- [4] Batista Milan 2014 Analytical treatment of equilibrium configurations of cantilever under terminal loads using jacob elliptical functions. *International Journal of Solids and Structures*, 51(13): 2308–2326
- [5] Corre Grégoire, Lebée Arthur, Sab Karam, Ferradi M K and Cespedes X 2020 A new higher-order elastoplastic beam model for reinforced concrete. *Meccanica*, 55(4): 791–813
- [6] Bathe Klaus-Jürgen and Bolourchi Said 1980 A geometric and material nonlinear plate and shell element. *Computers & structures*, 11(1-2): 23–48
- [7] Spaone Enrico, Filippou Filip C and Taucer Fabio F 1996 Fibre beam–column model for non-linear analysis of r/c frames: Part i. formulation. *Earthquake Engineering & Structural Dynamics*, 25(7): 711–725

- [8] Feng De-Cheng and Xu Jun 2018 An efficient fiber beam-column element considering flexure–shear interaction and anchorage bond-slip effect for cyclic analysis of rc structures. *Bulletin of Earthquake Engineering*, 16(11): 5425–5452
- [9] Nallathambi Ashok Kumar, Lakshmana Rao C and Srinivasan Sivakumar M 2010 Large deflection of constant curvature cantilever beam under follower load. *International Journal of Mechanical Sciences*, 52(3): 440–445
- [10] Chen Li 2010 An integral approach for large deflection cantilever beams. *International Journal of Non-Linear Mechanics*, 45(3): 301–305
- [11] Lofrano Egidio, Paolone Achille and Ruta Giuseppe 2013 A numerical approach for the stability analysis of open thin-walled beams. *Mechanics Research Communications*, 48: 76–86
- [12] Bui Nghia Nam, Ngo M, Nikolic M, Brancherie Delphine and Ibrahimbegovic A 2014 Enriched timoshenko beam finite element for modeling bending and shear failure of reinforced concrete frames *Computers & Structures*, 143: 9–18
- [13] Paulo João 2015 Pascon Numerical analysis of highly deformable elastoplastic beams. *Latin American Journal of Solids and Structures*, 12(8): 1595–1615
- [14] Bitar Ibrahim, Grange Stéphane, Kotronis Panagiotis and Benkemoun Nathan 2018 A comparison of displacement-based timoshenko multi-fiber beams finite element formulations and elasto-plastic applications. *European Journal of Environmental and Civil Engineering*, 22(4): 464–490
- [15] Corre Grégoire, Lebée Arthur, Sab Karam, Ferradi Mohammed Khalil and Cespedes Xavier 2018 The asymptotic expansion load decomposition elastoplastic beam model. *International Journal for Numerical Methods in Engineering*, 116(5): 308–331
- [16] Gardiner Frank J 1957 The springback of metals. *Trans. ASME*, 79(1): 1–9
- [17] Hu Jack, Marciniak Zdzislaw and Duncan John 2002 *Mechanics of sheet metal forming*. Elsevier
- [18] Natarajan A and Peddieson J 2011 Simulation of beam plastic forming with variable bending moments. *International Journal of Non-Linear Mechanics*, 46(1): 14–22
- [19] Sazonov Edward and Klinkhachorn Powsiri 2005 Optimal spatial sampling interval for damage detection by curvature or strain energy mode shapes. *Journal of sound and vibration*, 285(4-5): 783–801
- [20] Ciambella J and Vestroni F 2015 The use of modal curvatures for damage localization in beam-type structures. *Journal of Sound and Vibration*, 340: 126–137
- [21] Khiem Nguyen Tien 2020 Mode shape curvature of multiple cracked beam and its use for crack identification in beam-like structures. *Vietnam Journal of Mechanics*
- [22] Chiorean C G 2013 A computer method for nonlinear inelastic analysis of 3d composite steel–concrete frame structures. *Engineering Structures* 57: 125–152
- [23] Chiorean Cosmin G 2017 A computer method for moment-curvature analysis of composite steel-concrete cross-sections of arbitrary shape. *Engineering Structures and Technologies*, 9(1): 25–40
- [24] Dhakal Suresh and Moustafa Mohamed A 2019 Mc-bam: Moment–curvature analysis for beams with advanced materials *SoftwareX* 9: 175–182
- [25] Yoo Doo-Yeol, Banthia Nemkumar and Yoon Young-Soo 2017 Experimental and numerical study on flexural behavior of ultra-high-performance fiber-reinforced concrete beams with low reinforcement ratios. *Canadian Journal of Civil Engineering*, 44(1): 18–28
- [26] Oller Sergio and Barbat Alex H 2006 Moment–curvature damage model for bridges subjected to seismic loads. *Computer Methods in Applied Mechanics and Engineering*, 195(33-36): 4490–4511
- [27] Brojan Miha, Videnic T and Kosel Franc 2009 Large deflections of nonlinearly elastic non-prismatic cantilever beams made from materials obeying the generalized ludwick constitutive law. *Meccanica*, 44(6): 733–739
- [28] Liu Hua, Han Yi and Yang Jialing 2017 Large deflection of curved elastic beams made of ludwick type material. *Applied Mathematics and Mechanics*, 38(7): 909–920, 2017.
- [29] Patel Bhakti N, Pandit D and Srinivasan Sivakumar M 2017 Moment-curvature based elasto-plastic model for large deflection of micro-beams under combined loading. *International Journal of Mechanical Sciences*, 134: 158–173
- [30] Pandit Debojyoti and Srinivasan Sivakumar M 2020 Simulation of shape memory cycle of a polymeric beam undergoing large deflection using a simple incremental approach. *Journal of Intelligent Material Systems and Structures*, 31(4): 515–524
- [31] Pandit D and Srinivasan Sivakumar M 2016 An incremental approach for springback analysis of elasto-plastic beam undergoing contact driven large deflection. *International Journal of Mechanical Sciences*, 115: 24–33
- [32] Pandit D and Chakraborty S 2019 Simulation of pseudo-elastic effect in a shape memory alloy beam. In: *Proceedings of the 64th Congress of The Indian Society of Theoretical and Applied Mechanics*, Indian Institute of Technology, Bhubaneswar, India, December 9-12
- [33] Simo Juan C and Hughes Thomas J R 2006 *Computational inelasticity*, volume 7. Springer Science & Business Media
- [34] Pandit D, Thomas N, Patel Bhakti and Srinivasan S M 2015 Finite deflection of slender cantilever with predefined load application locus using an incremental formulation. *CMC*, 45, no. 2: 127–144
- [35] Chen Wai-Fah and Han Da-Jian 2007 *Plasticity for structural engineers J. Ross Publishing*